Supplemental material

Imaging Data acquisition

All functional MRI (fMRI) data were acquired using a 3.0 Tesla scanner (Siemens, Verio, Germany) in Dongzhimen Hospital, Beijing University of Chinese Medicine, under the following imaging conditions: (1) T2WI Gradient Echo-Planar Imaging (EPI) sequence: repetition time (TR) = 2,000 ms, echo time (TE) = 30 ms, field of view = 225 mm × 225 mm, matrix = 64 × 64, flip angle = 90°, slice thickness = 3.5 mm, slices = 31. (2) 3D-T1WI sequence: TR = 1,900 ms, TE = 2.52 ms, field of view = 256 mm × 256 mm, matrix = 256 × 256, flip angle = 9°, slice thickness = 1.0 mm, slices = 176. The scanning protocol aimed to investigate the effect of acupuncture on the central nervous system with an unrepeatable event-related experimental design. Ischaemic stroke (IS) patients accepted two scans before and after acupuncture and healthy controls (HCs) accepted one scan following the scanning steps: (1) The BOLD scanning lasted for 8 min 10 s, in which all participants were instructed to remain awake, relax with their eyes closed, remain motionless, and try to think about nothing. (2) High-resolution T1 structural image scanning lasted for 4 min 10 s.

Neuroimaging processing

Data pre-processing was conducted by SPM12 (http://www.fil.ion.ucl.ac.uk/spm) package based on MATLAB 2023a, including converting EPI and T1 DICOM to NIFTI, discarding the first 10 volumes, slicing timing, realigning head motion within 2 mm or 2°, normalizing to the Montreal Institute of Neurology (MNI) space with resampling to 3 × 3 × 3 mm^3, smoothing with a Gaussian kernel of 6 × 6 × 6 mm^3 full width at half-maximum, and detrending, filtering with a bandpass from 0.01 to 0.08 Hz, removing covariates. In particular, given the symmetrical distribution of sensorimotor network and cerebellar network connected through the corpus callosum bilaterally, we defined the left hemisphere as the affected side and the right hemisphere as the intact side by flipping the right-lesion images to the left.

Static functional data operation, applying DPARSF 5.4 (http://resting-fmri.sourceforge.net), adopt voxel-mirrored homotopic connectivity (VMHC) and static functional connectivity (sFC) analysis based on region of interest (ROI) to reflect interhemispheric information integration bilaterally and specific regions' connectivity with the whole brain. Firstly, the normalization based on a symmetric T1 template, created by averaging the mean T1 template from each subject's T1 image in MNI space with its flipped version, was applied to transform the functional data to calculate the VMHC values via Pearson correlation and Fisher Z transformation. Secondly, we defined the regions with statistical differences on VMHC as ROIs and obtained their sFC values to investigate the intrinsic bilaterally pathological patterns of functional connectivity on voxel level.

Dynamic functional connectivity (DFC) indicators, operated on Dynamic BC 2.2, were coefficient of variability of VMHC (CV_VMHC) and time attributes based on K-means clustering. Sliding-window analysis was employed to research the characteristic bilateral transformation of brain and reveal the curative mechanisms of acupuncture, with window size set as 30TR and window step as 1TR.[1] Subsequently we gained the CV_VMHC partially and the DFC states of clustering accompanied with fraction time (FT), mean dwell time (MDT) and number of transitions (NT) on whole level.

Controlling for Head Motion

We verified the absence of severe motion by calculating individual mean and maximum framewise displacements (FD) to control any underlying effects.[2-3] Participants with a mean FD > 0.5 mm or maximum FD > 1 mm were excluded according to clinical neuroimaging studies.[4-5] Finally, 46 ISs and 34 HCs were selected for the per-protocol analysis. There was no significant difference in FD between the HC group (mean ± SD = 0.10 ± 0.060 mm) and the IS group (mean ± SD = 0.11 ± 0.060 mm, $P = 0.554$).

Table

TABLE S1 | Acupoints Location of acupuncture*

Acupoint	Meridian	Location
Hegu (LI4)	Large Intestine Meridian (LI)	On the dorsum of the hand, radial to the midpoint of the second metacarpal bone.
Neiguan (PC6)	Pericardium Meridian (PC)	On the anterior aspect of the forearm, between the tendons of the palmaris longus and the flexor carpi radialis, 2 B-cun† proximal to the palmar wrist crease.
Quchi (LI11)	Large Intestine Meridian (LI)	On the lateral aspect of the elbow, at the midpoint of the line connecting LU5 with the lateral epicondyle of the humerus.
Zusanli (ST36)	Stomach Meridian (ST)	On the anterior aspect of the leg, on the line connecting ST35 with ST41, 3 B-cun inferior to ST35.
Yanglingquan (GB34)	Gallbladder Meridian (GB)	On the fibular aspect of the leg, in the depression anterior and distal to the head of the fibula.
Sanyinjiao (SP6)	Spleen Meridian (SP)	On the tibial aspect of the leg, posterior to the medial border of the tibia, 3 B-cun superior to the prominence of the medial malleolus.

1

* Acupoints located on meridians.[6-8]

† B-cun, bone proportional cun. According to the measurements of body parts based on Gudu from *Yellow Emperor's Canon of Medicine · Spiritual Pivot*, the method is to divide the length between two points of particular joints into equal portions, and each portion is equivalent to 1 B-cun.

TABLE S2 | Non-acupoints location of acupuncture*

Non-acupoint	Location
NA_LI4	1 F-cun† radial to the LI4.
NA_PC6	1 F-cun ulnalr to the PC6.
NA_LI11	1 F-cun anterior to the LI11.
NA_ST36	1 F-cun fibular to the ST36.
NA_GB34	1 F-cun tibial to the GB34.
NA_SP6	1 F-cun posterior to the SP6.

2

* Non-acupoints located lateral or medial to meridians. NA, non-acupoint.

† F-cun, finger cun. It's defined as the width of the interphalangeal joint of patient's thumb. 1F-cun = 20 mm.[7,9-10]

TABLE S3 | Regions reported significant differences on VMHC between IS and HC group in preacupuncture stage*

Region† (L/R)	Voxel	MNI coordinate‡			Intensity values
		x	y	z	
All subjects					
Heschl_R	13	42	-18	15	-4.32789
Heschl_L	13	-42	-18	15	-4.32789
Cerebellum_Crus1_R	40	27	-72	-27	-4.75086
Cerebellum_Crus1_L	40	-27	-72	-27	-4.75086
Cerebellum_Crus2_R	11	45	-66	-48	-4.00509
Cerebellum_Crus2_L	11	-45	-66	-48	-4.00509
Postcentral_R	4	57	0	21	-3.92303
Postcentral_L	4	-57	0	21	-3.92303
Mild to moderate subjects					
Postcentral_L	13	-57	0	36	-4.84073
Postcentral_R	12	57	0	36	-4.84073
Cerebellum_Crus1_R	14	27	-69	-27	-3.96934
Cerebellum_Crus1_L	14	-27	-69	-27	-3.96934
Severe subjects					
Cerebellum_Crus1_R	8	45	-69	-33	-4.13129
Cerebellum_Crus1_L	8	-45	-69	-33	-4.13129
Cerebellum_6_R	7	21	-63	-18	-4.44123
Cerebellum_6_L	7	-21	-63	-18	-4.44123

3

* VMHC values were statistically different between the ISs and the HCs within severity subgroups in preacupuncture stage. The statistical significance was inspected by two-sample t-test with Gaussian random field (GRF) multiple comparisons, setting thresholds as the voxel level $P<0.001$ and the cluster level $P<0.05$. HC, healthy control; IS, ischaemic stroke; VMHC, voxel-mirrored homotopic connectivity.

† The reported regions referred to anatomical automatic labeling template.

‡ MNI, Montreal Neurological Institute.

TABLE S4 | Significant differences on FM scores between IS group and HC group in each acupuncture treatment stage*

	FM, median (IQR), scores		*z*	*P* value†
	Preacupuncture	Postacupuncture		
The HA group				
All subjects				
FM-UE	46.00 (13.30 − 65.00)	58.00 (26.00 − 65.00)	4.362	0.000
FM-LE	30.50 (23.30 − 33.00)	32.00 (29.30 − 34.00)	3.851	0.000
FM	74.00 (42.80 − 95.80)	88.50 (57.30 − 99.00)	4.628	0.000
Mild to moderate subjects				
FM-UE	60.50 (46.00 − 65.00)	63.50 (57.30 − 66.00)	3.356	0.001
FM-LE	32.00 (29.00 − 33.00)	33.00 (32.00 − 34.00)	2.919	0.004
FM	89.00 (77.00 − 98.30)	95.00 (89.30 − 99.00)	3.731	0.000
Severe subjects				
FM-UE	8.50 (7.00 − 11.80)	12.50 (9.30 − 23.80)	2.812	0.005
FM-LE	22.50 (15.80 − 25.50)	26.00 (18.30 − 30.50)	2.533	0.011
FM	31.50 (30.00 − 39.30)	40.50 (32.50 − 54.30)	2.807	0.005
The NA group				
FM-UE	57.50 (20.30 − 64.30)	62.00 (36.30 − 65.00)	2.185	0.029
FM-LE	30.50 (24.00 − 34.00)	33.00 (30.30 − 34.00)	2.659	0.008
FM	85.000(45.00 − 97.30)	94.000(62.80 − 98.30)	2.661	0.008

4

* There were statistically significant difference between the preacupuncture and postacupuncture stage. FM, Fugl-Meyer; HA, hand-foot 12 needles acupuncture; HC, healthy control; IS, ischaemic stroke; LE, lower extremity; NA, non-acupoint; UE, upper extremity.

† Paired Wilcoxon test.

TABLE S5 | Regions reported significant differences on VMHC associated with HA group in postacupuncture stage*

Region† (L/R)	Voxel	MNI coordinate‡			Intensity values
		x	y	z	
HA group vs HCs					
All subjects					
Precentral_L	52	-57	-3	33	-5.41316
Postcentral_R	51	57	-3	33	-5.41316
Cingulum_Mid_L	14	-6	-9	42	-4.96266
Precentral_R	11	48	-15	42	-4.08350
Postcentral_L	10	-48	-15	42	-4.08350
Cingulum_Mid_R	8	6	-9	42	-4.96266
Cerebellum_6_R	7	36	-48	-27	-4.58769
Cerebellum_6_L	6	-36	-48	-27	-4.58769
Cerebellum_Crus1_R	5	15	-78	-24	-4.52599
Cerebellum_Crus1_L	5	-15	-78	-24	-4.52599
Mild to moderate subjects					
Postcentral_R	36	57	-3	30	-6.00771
Precentral_L	36	-57	-3	30	-6.00771
Temporal_Sup_R	34	63	-6	6	-5.29370
Temporal_Sup_L	19	-63	-6	6	-5.29370
Cingulum_Mid_L	12	-9	-6	36	-4.48257
Cingulum_Mid_R	6	6	-9	42	-4.09427
Supp_Motor_Area_R	6	9	-9	63	-4.72219
HA group vs NA group					
Mild to moderate subjects					
Cerebellum_8_L	3	-36	-48	-57	4.46577

5

* VMHC values were statistically different when HA group compared to the HCs or NA group within severity subgroups in postacupuncture stage. The statistical significance was inspected by two-sample t-test with GRF multiple comparisons, setting thresholds as the voxel level $P<0.001$ and the cluster level $P<0.05$. HA, hand-foot 12 needles acupuncture; HC, healthy control; NA, non-acupoint; VMHC, voxel-mirrored homotopic connectivity.

† The reported regions referred to anatomical automatic labeling template.

‡ MNI, Montreal Neurological Institute.

TABLE S6 | Regions reported significant differences on VMHC with their bilateral sFC between preacupuncture and postacupuncture stage in HA group*

Region† (L/R)	Voxel	MNI coordinate‡			Intensity values
		x	y	z	
VMHC§					
Frontal_Sup_Orb_R	10	27	63	-6	4.95783
Frontal_Sup_Orb_L	10	-27	63	-6	4.95783
sFC_Frontal_Sup_Orb_R‖					
Frontal_Sup_Orb_L	11	-24	63	-6	5.13648
Cerebellum_6_R	8	18	-69	-21	4.47169
Frontal_Sup_Medial_R	8	3	60	3	4.38550
Occipital_Sup_L	7	-9	-99	9	4.67775
sFC_Frontal_Sup_Orb_L‖					
Frontal_Mid_Orb_R	27	33	60	-9	4.42451
Frontal_Sup_Orb_R	17	18	63	-6	5.27338
SupraMarginal_R	17	60	-36	24	-5.09594
Temporal_Sup_L	10	-51	-33	21	-5.97007
Cerebellum_7b_R	5	33	-66	-45	4.40150
Cerebellum_6_R	5	30	-72	-24	4.42451
CV_VMHC§					
Cingulum_Post_R	6	3	-27	24	-4.86718
Cingulum_Post_L	6	-3	-27	24	-4.86718

6

* VMHC and its variability were compared between the preacupuncture and postacupuncture stage to identify the ROIs, so as to investigate the therapeutically bilateral effects on neural plasticity of acupuncture. CV_VMHC, coefficient of variability of VMHC; HA, hand-foot 12 needles acupuncture; sFC, static functional connectivity; VMHC, voxel-mirrored homotopic connectivity.

† The reported regions referred to anatomical automatic labeling template.

‡ MNI, Montreal Neurological Institute.

§ Paired t-test was adopt with GRF multiple comparisons, setting thresholds as the voxel level $P<0.001$ and the cluster level $P<0.05$.

‖ Two-sample t-test in static functional connectivity analysis with the bilateral Frontal_Sup_Orb as ROIs.

TABLE S7 | Regions reported significant differences on time attributes of DFC between preacupuncture and postacupuncture stage in HA group*

DFC state	MDT/FT, mean (SD), seconds		*t*	*P* value†
	Preacupuncture	Postacupuncture		
FT_pre_S1 - FT_post_S1	0.03 (0.18)	0.33 (0.30)	-4.413	0.000
FT_pre_S2 - FT_post_S2	0.39 (0.33)	0.67 (0.30)	-3.253	0.003
MDT_pre_S1 - MDT_post_S1	5.63 (30.86)	34.59 (41.65)	-2.920	0.007
MDT_pre_S2 - MDT_post_S2	40.54 (44.17)	74.83 (55.30)	-2.590	0.015

7

* There were statistically significant difference between the preacupuncture and postacupuncture stage. DFC, dynamic functional connectivity; FT, fraction time; HA, hand-foot 12 needles acupuncture; MDT, mean dwell time.

† Paired t-test.

Figure

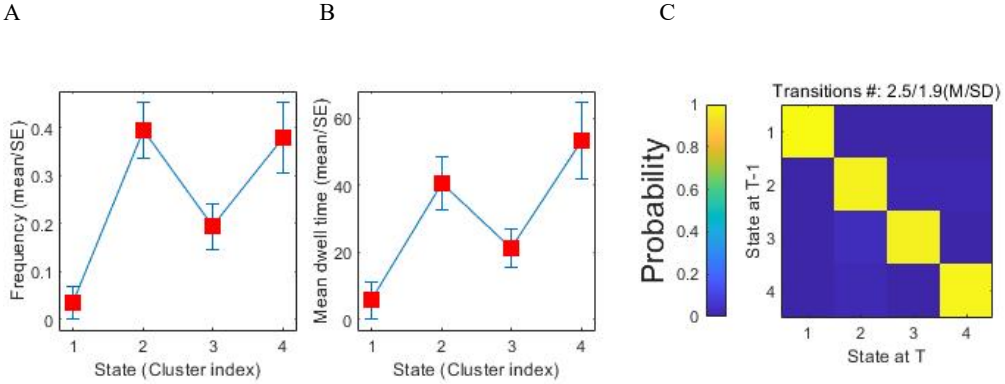

Figure S1 | The time attributes of DFC in preacupuncture stage. (A) The FT of each dynamic state in preacupuncture stage. (B) The MDT of each dynamic state in preacupuncture stage. (C) The NT of dynamic states in preacupuncture stage. DFC, dynamic functional connectivity; FT, fraction time; MDT, mean dwell time; NT, number of transitions.

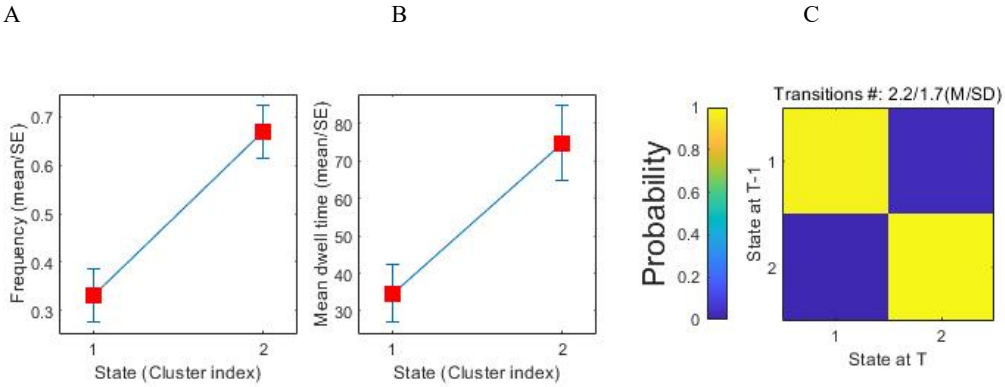

Figure S2 | The time attributes of DFC in postacupuncture stage. (A) The FT of each dynamic state in postacupuncture stage. (B) The MDT of each dynamic state in postacupuncture stage. (C) The NT of dynamic states in postacupuncture stage. DFC, dynamic functional connectivity; FT, fraction time; MDT, mean dwell time; NT, number of transitions.

REFERENCES

1 Favaretto C, Allegra M, Deco G, *et al*. Subcortical-cortical dynamical states of the human brain and their breakdown in stroke. *Nat Commun* 2022;**13**:5069.

2 Hutchison RM, Womelsdorf T, Allen EA, *et al*. Dynamic functional connectivity: promise, issues, and interpretations. *Neuroimage* 2013;**80**:360-378.

3 Power JD, Mitra A, Laumann TO, *et al*. Methods to detect, characterize, and remove motion artifact in resting state fMRI. *Neuroimage* 2014;**84**:320-341.

4 Yu Q, Yin D, Kaiser M, *et al*. Pathway-Specific Mediation Effect Between Structure, Function, and Motor Impairment After Subcortical Stroke. *Neurology* 2023;**100**:e616-e626.

5 Lu M, Du Z, Zhao J, *et al*. Neuroimaging mechanisms of acupuncture on functional reorganization for post-stroke motor improvement: a machine learning-based functional magnetic resonance imaging study. *Front Neurosci* 2023;**17**:1143239.

6 Beijing Hospital of Traditional Chinese Medicine. Gold Needle Wang Leting. Beijing: *Beijing Publishing House*, 1984.

7 Standardization administration. Nomenclature and location of meridian points. Beijing: *Inspection and Quarantine of the People's Republic of China*, 2021.

8 WHO Regional Office for the Western Pacific. WHO Standard Acupuncture Point Locations in the Western Pacific Region. Manila: *World Health Organization*, 2009.

9 Liu Z, Liu Y, Xu H, *et al*. Effect of Electroacupuncture on Urinary Leakage Among Women With Stress Urinary Incontinence: A Randomized Clinical Trial. *JAMA* 2017;**317**:2493-2501.

10 Wang Y, Yang JW, Yan SY, *et al*. Electroacupuncture vs Sham Electroacupuncture in the Treatment of Postoperative Ileus After Laparoscopic Surgery for Colorectal Cancer: A Multicenter, Randomized Clinical Trial. *JAMA Surg* 2023;**158**:20-27.